12-1-2006

Local Buckling Analysis of Trapezoidal Rib Orthotropic Bridge Deck Systems

Matthew T. Yarnold

John L. Wilson

Wan-Chun Jen

Ben T. Yen

Local Buckling Analysis of Trapezoidal Rib Orthotropic Bridge Deck Systems

by

Matthew T. Yarnold

John L. Wilson

Wan-Chun Jen

Ben T. Yen

ATLSS Report No. 06-27

ATLSS is a National Center for Engineering Research on Advanced Technology for Large Structural Systems

117 ATLSS Drive
Bethlehem, PA 18015-4729

Phone: (610)758-3525
Fax: (610)758-5902

www.atlss.lehigh.edu
Email: inatl@lehigh.edu

Local Buckling Analysis of Trapezoidal Rib Orthotropic Bridge Deck Systems

MATTHEW T. YARNOLD[1]*, JOHN L. WILSON[2], WAN-CHUN JEN[3], and BEN T. YEN[2]

1. Ammann & Whitney, 2300 Chestnut Street, Philadelphia, PA 19103, USA

2. Department of Civil and Environmental Engineering, 13 E. Packer Avenue, Fritz Engineering Laboratory, Lehigh University, Bethlehem, PA 18015, USA

3. Jacobs Civil, 70 Wood Avenue South, 4th Floor, Iselin, NJ 08830, USA

This paper analyzes the behavior of local buckling in trapezoidal rib orthotropic bridge deck systems. The primary objective of this paper is to compare the condition of a uniform stress pattern (column) and that of a nonuniform stress pattern (beam-column). The former is current practice while the latter is recommended based on the current study. The presence of thin steel plate members within the deck system causes local buckling to be a valid concern. Parametric analyses were performed using the finite element method to examine local buckling of the rib walls (webs) and deck plate by varying the corresponding width-to-thickness ratios. Since the rib walls have the highest width-to-thickness ratio, they were the primary focus of this research. Generally, this type of deck system is analyzed under axial compression due to global forces. However, bending moments from the local loading of the deck weight and vehicles are typically present in the system. Therefore, the bridge deck system was analyzed under axial compression and negative bending moment for local buckling in the rib walls. The results demonstrate a reduction in the capacity of the deck system at which local buckling is initiated in the rib walls due to the existence of negative bending moment near the floorbeams in addition to the global axial forces.

Keyword: Orthotropic Deck; Bridge; Local buckling; Deck; Rib; Finite Element Analysis

1. Introduction

Components of orthotropic bridge deck systems are typically studied under axial compression to simulate forces in the deck due to the global action of the bridge (Wolchuk 1963, Chen & Duan 1999, AASHTO 2004). However, local bending moments due to the dead weight of the deck and vehicular loading are contributing factors of the local buckling behavior within the system. For that reason, a study was conducted using finite element analysis to better understand the occurrence of local buckling in critical components of the system.

Orthotropic bridge decks are a steel decking system typically utilized in long-span bridges including; box, plate girder, arch, suspension, movable, and cable stayed bridges.

* Corresponding author. Email: MYarnold@ammann-whitney.com

One of the primary reasons for the use of an orthotropic deck is that it offers a relatively low weight decking system which requires minimal future maintenance. For that reason, many existing bridges have their original heavier deck replaced with a panelized prefabricated orthotropic deck system. Another advantage of redecking with this type of system is that it provides uninterrupted use (at peak traffic demand) during the replacement of the bridge deck, plus higher live load capacity.

In general, orthotropic bridge decks are comprised of a steel deck plate stiffened by longitudinal rib members at right angles, or orthogonal, to the floorbeams. The deck plate and the longitudinal stiffeners are continuous over the floorbeams. The longitudinal stiffeners are of the "open rib" or "closed rib" type (Troisky 1987, Wolchuk 1963, AASHTO 2004). The open ribs are outstanding plates, angles or tees attached under the deck plate and are torsionally soft. The closed ribs are troughs of trapezoidal, triangular or curved cross section which are torsionally stiff. At the present, the most widely used system is the closed rib type, shown in Figure 1. The high torsional resistance of the closed ribs allows the floorbeams to be spaced at a greater distance. The most commonly used shape for closed rib stiffeners of orthotropic decks in the USA is the trapezoidal shaped rib which is the type analyzed in this study.

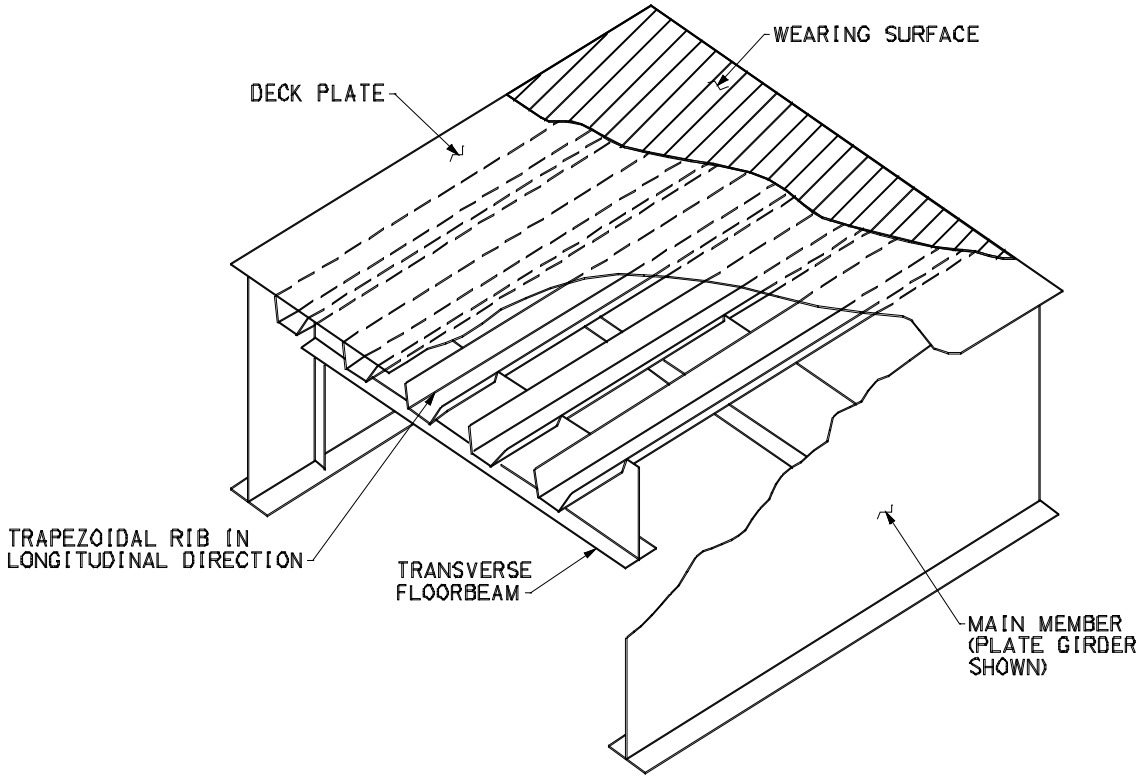

Figure 1. Closed rib orthotropic bridge deck system featuring trapezoidal shaped ribs

In recent years the development of fatigue cracks at the junction of the deck plate, floorbeam and trapezoidal ribs has led to extended studies of these connections. Cut-outs in floorbeam webs are commonly introduced for the alignment of the ribs and for facilitating welding at the connection. One detailing requirement of closed rib orthotropic

bridge deck is to "make the rib web relatively slender compared to the deck plate" (AASHTO C.9.8.3.7.2). This condition of slender webs of the trapezoidal rib stiffeners and the continuity of the deck plate and ribs over the floorbeams make the ribs subject to negative bending at the floorbeams. At these locations, the lower portion of the relatively slender ribs is subjected to a higher compressive stress than the average compressive stress of the rib. The local buckling strength could be lower than that computed for uniform compressive stress. The comparison of local buckling of the components of orthotropic deck panels at floorbeams under these two conditions of stresses is the goal of this study.

2. Analytical Approach

This study investigates local buckling within a trapezoidal rib orthotropic bridge deck system. A comparison is made between local buckling of the rib walls and deck plate subjected to specific stress distributions (explained in Sections 4 and 5). The location of initial local buckling within the deck cross-section was of importance to the study. A cross-section of the trapezoidal ribs and the deck plate at a floorbeam is sketched in Figure 2 with the corresponding notation. In many cases, the distance between the walls of the ribs (a) and between two ribs (e) is the same. This arrangement makes the design process simpler; however it is not required by AASHTO. In addition, the plate slenderness ratio of the deck plate (a/t_d and e/t_d) is lower than that of the rib walls ($h`/t_r$). Consequently, the local buckling strength of the rib walls is lower than that of the deck plate, and is, therefore, the primary concern.

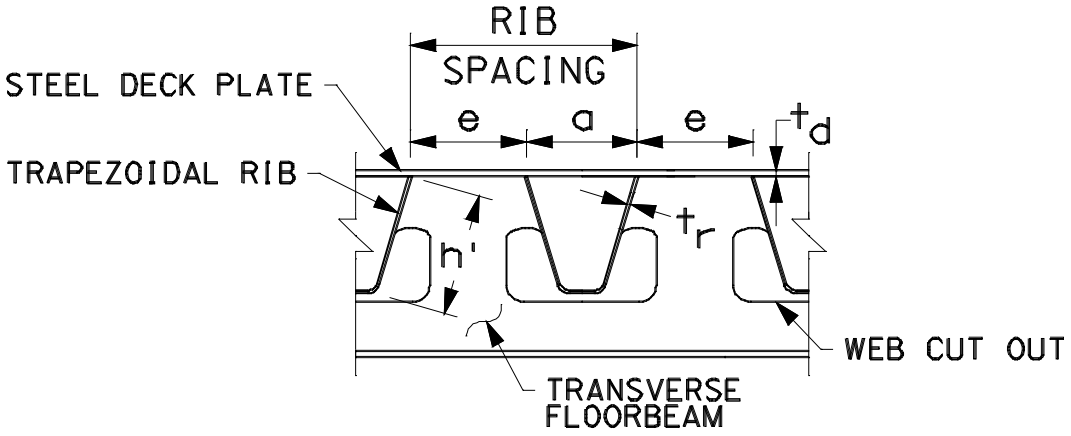

Figure 2. Trapezoidal rib cross-section and notation

Components of orthotropic deck systems are subjected to a variety of stress distributions which depend on the bridge type, the loading conditions and the location of vehicular loads on the deck. At cross-sections of orthotropic bridge decks the trapezoidal ribs are subjected to high compressive forces due to global action of the structure and localized forces due to the dead weight and vehicular loading. Since the longitudinal ribs are continuous through the floorbeams localized negative bending of the ribs is present at the floorbeam locations. For that reason, this study analyzed trapezoidal ribs of orthotropic

bridge decks subjected to a non-uniform stress distribution with the maximum compressive stress at the bottom of the rib.

For illustration, Figure 3 shows an elevation view of a continuous rib of an orthotropic deck in a plate girder bridge. The global action of the bridge generates a compressive stress distribution in the ribs similar to that shown in Figure 4 (a). Combining this stress distribution with that at cross-section A-A from the local forces (Figure 4 (b)) results in a superimposed stress distribution of Figure 4 (c) (Wolchuk, 1963). The rib walls at cross-section A-A are not subjected to uniform stress but rather to higher compressive stress at the bottom of the rib. Local buckling of the rib and deck components were analyzed in this study under the superimposed compressive stress distribution. For comparison, local buckling of the rib walls and deck plate was also analyzed under a uniform compressive stress distribution.

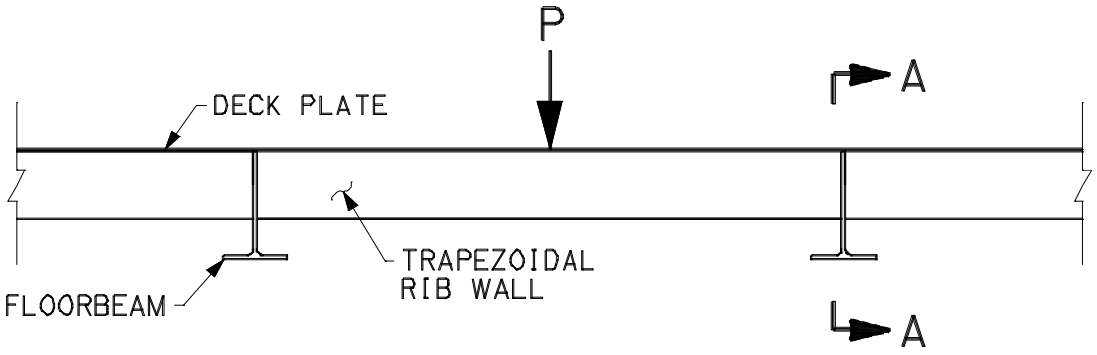

Figure 3. Elevation view of continuous trapezoidal rib

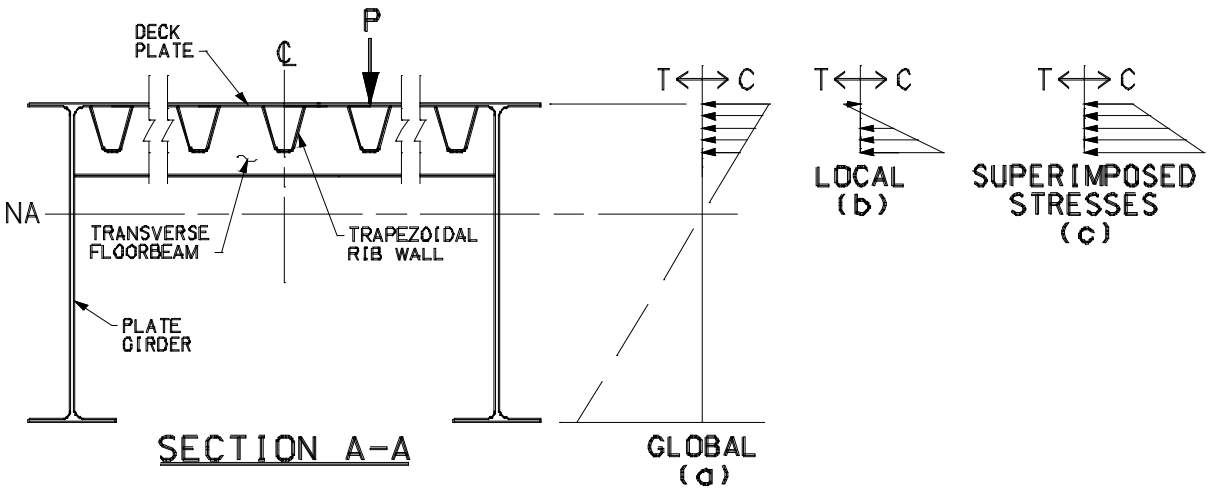

Figure 4. Section A-A (a) Global stress distribution (b) Local stress distribution (c) Superimposed stress distribution in rib members

In the analysis by the finite element method, the plate width (a or e and h`) and thickness (t_d and t_r) were the primary parameters. Other factors such as geometric

imperfections and residual stresses (Chen & Yang, 2002) were not included in the analysis of local buckling. This is due to the fact that the study is not an attempt to indicate the load carrying strength of the ribs or the deck plate. The parametric study investigates local buckling behavior under the uniform and non-uniform stress distributions explained above. Then, qualitative conclusions are drawn from comparing local buckling of the rib walls and deck plate under the different stress distributions.

3. Verification of the Finite Element Model

The adequacy of the finite element model (FEM) was confirmed by a comparison of the FEM results with physical test results in a related project (Jen and Yen, 2006). That project tested parts of an orthotropic deck panel which were cut from a prototype of the Bronx-Whitestone Bridge (BWB) replacement deck in New York City (Tsakopoulos and Fisher, 2005). The rib specimens were loaded under axial compression along with a transverse load (Figure 5). The FEM of the rib tests used the same software (ABAQUS, 2002) and modeling techniques as in this parametric study. Overall, the results from the FEM and the test specimens displayed high correlation, and verified the accuracy of the finite element model of this study.

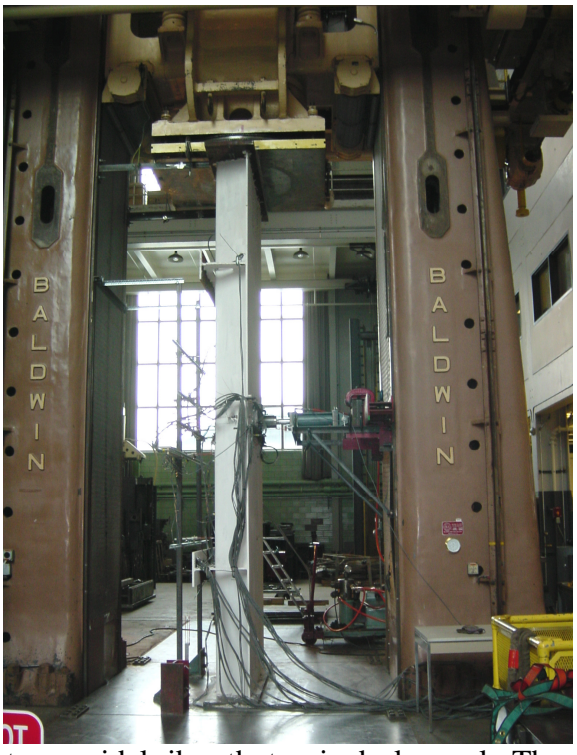

Figure 5. Testing of a trapezoidal rib orthotropic deck panel. The specimen is positioned vertically in the "Baldwin" machine.

The most important results from the comparison between the test results and the FEM of this study were the failure mode and location. The tested specimens, with the inherent residual stresses, sustained inelastic local buckling in the rib walls after the onset of

yielding as was also indicated by the results of the finite element analysis without considering residual stresses. Local buckling initiated at the lower end of the test ribs and of the FEM (Figure 6). With this confirmation, and for the reason that residual stresses vary with rib dimension and are tedious to be incorporated in a parametric study, the residual stresses were omitted in the comparative investigations of this study.

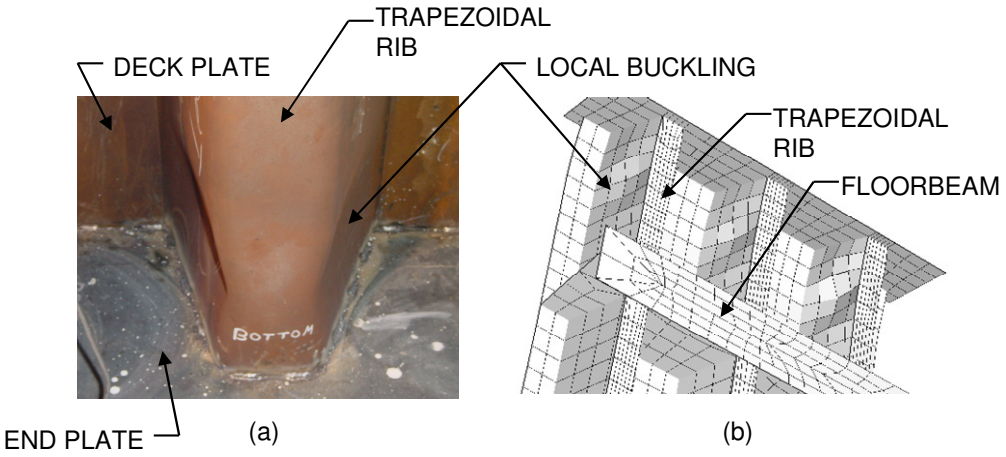

Figure 6. Inelastic local buckling of the rib walls of (a) a test specimen and (b) the finite element model (viewed from below)

4. Parameters and Loading

The trapezoidal rib orthotropic bridge deck parametric study was performed on a five rib segment of a deck panel. A five rib segment provided sufficient width for the examination of localized failure (local buckling) of the rib wall and deck plate. The geometric parameters were varied from the cross sectional dimensions of the base model (from BWB) and are shown in Figure 7. However, the dimensions are simply used as a starting point for the comparative parametric analysis on trapezoidal ribs of orthotropic bridge decks. The floorbeam cut-out detail was omitted in the finite element models. The cut-out is primarily for the improvement of fatigue strength at the connection, and has negligible effects toward local buckling of the rib walls or deck plate (Chen & Duan 1999, Connor 2002, Galambos 1998).

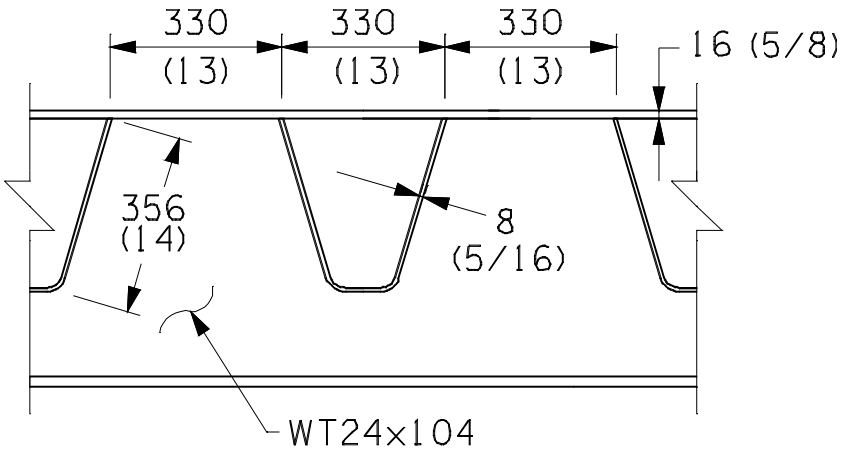

Figure 7. Orthotropic deck cross-sectional dimensions for the base model (units: millimeters (inches)*)

A non-linear static analysis was performed using the finite element model. The mechanical properties of the Grade 50 steel plates were obtained from the previously conducted project (Jen and Yen, 2005). The stress-strain curve used is shown below in Figure 8.

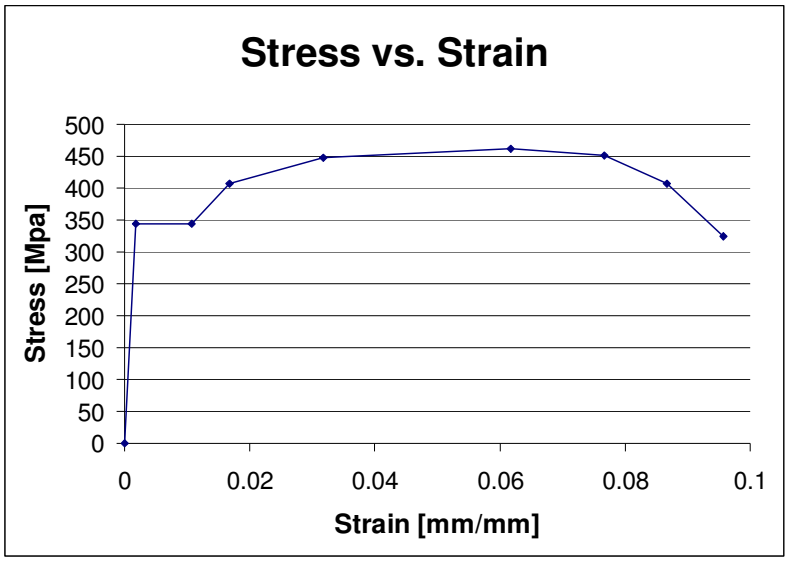

Figure 8 – Stress-Strain Relationship

The geometric parameters of analysis were the width and thickness of the plate components. The depth and thickness of the rib walls (h` and t_r), the thickness of the deck plate (t_d), and the distance between the rib walls (a and e) were varied from the basic case. Table 1 shows the values of these parameters and the corresponding plate slenderness ratios

* Note: The exact units used in this research were English units. The approximate metric equivalent is also given throughout the paper.

($h`/t_r$ and a/t_d or e/t_d). It is noted that a wide range of widths and thicknesses were analyzed to cover a full range of the slenderness ratio. Therefore, the local buckling behavior could be better compared.

Table 1. Parameters and Slenderness Ratios (*base model)

(a) Axial Load with End Moments (Beam - Columns)

t_r / h'	2.4 (3/32)	3.2 (1/8)	4.8 (3/16)	6.4 (1/4)	7.9 (5/16)	9.5 (3/8)	12.7 (1/2)	
356 (14)	149.3	112.0	74.7	56.0	44.8*	37.3	-	a = e = 330 (13)
394 (15.5)	165.3	124.0	82.7	62.0	49.6	41.3	31.0	t_d = 15.9 (5/8)
432 (17)	181.3	136.0	90.7	68.0	54.4	45.3	34.0	
t_d / a or e	3.2 (1/8)	4.8 (3/16)	6.4 (1/4)	9.5 (3/8)	12.7 (1/2)	15.9 (5/8)		
330 (13)	-	-	-	-	-	20.8*		h' = 356 (14)
381 (15)	120.0	80.0	60.0	40.0	30.0	24.0		t_r = 7.9 (5/16)
432 (17)	136.0	90.7	68.0	45.3	34.0	27.2		
483 (19)	152.0	101.3	76.0	50.7	38.0	30.4		

(b) Axial Load only (Columns)

t_r / h'	3.2 (1/8)	4.8 (3/16)	5.6 (7/32)	6.0 (15/64)	6.4 (1/4)	7.1 (9/32)	7.9 (5/16)	9.5 (3/8)	
356 (14)	112.0	74.7	64.0	59.7	56.0	49.8	44.8*	37.3	a = e = 330 (13) t_d = 15.9 (5/8)
t_d / a or e	6.4 (1/4)	7.9 (5/16)	9.5 (3/8)	11.1 (7/16)	12.7 (1/2)	14.3 (9/16)	15.9 (5/8)		
330 (13)	52.0	41.6	34.7	29.7	26.0	23.1	20.8*		h' = 356 (14) t_r = 7.9 (5/16)

Units: parameters in millimeters (inches)
Note: metric dimensions approximate (english dimensions exact)
* base model

Two separate loading conditions were applied. The first was that of a beam-column, to simulate the stress distribution of Figure 4 (c). A uniformly distributed compressive load was applied at the end of the deck segment through a loading block (Figure 9). The eccentricity between the centroid of the deck panel cross section and of the loading block produced an axial compressive force and negative bending moment. As a result, the compressive stresses within the deck segment are greater in the rib members than in the deck plate.

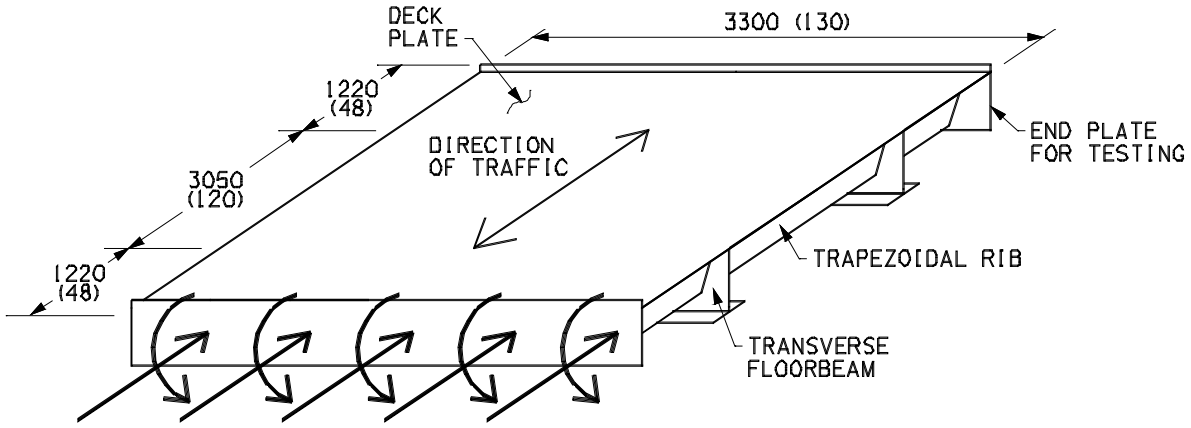

Figure 9. Loading applied to the five trapezoidal rib orthotropic deck finite element model - beam-column analysis (units: millimeters (inches))

The eccentricity was set so that the negative bending moment for the base model was approximately 2.5 times that produced from standard HL-93 loading (AASHTO, 2004) and 2.5 times for other parametric cases. The negative bending moment was magnified for several reasons. First, as mentioned above, the study focuses on the local buckling behavior under the two different stress distributions described in Section 2 not on the load carrying capacity of the system. The second reason is that the higher moments simulate the condition of permit vehicles crossing the structure. Another reason for increasing the applied bending moment is to compensate for the fact that residual stresses and geometric imperfections were not included in the comparative study.

The second loading condition was without eccentricity between centroids thus subjected the deck segment to a uniform compressive stress (Figure 10). Essentially, a trapezoidal rib of the deck segment was analyzed as a column, which is typical design practice.

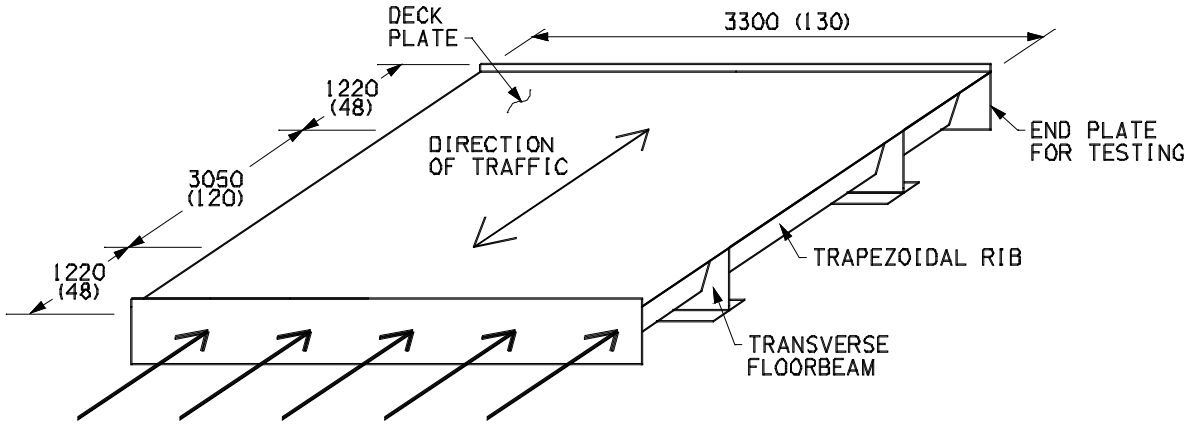

Figure 10 - Loading applied to the five trapezoidal rib orthotropic deck finite element model - column analysis (units: millimeters (inches))

5. Local Buckling Behavior

5.1 Beam-column analysis

Throughout the analysis the failure mode, failure location, variation of stresses, and magnitude of load at which local buckling occurred were examined. For each case analyzed in this study an axial load versus longitudinal displacement (shortening) curve was generated. Figure 11 shows two examples of load deflection curves which depict the behavior of the deck segment under the beam-column loading.

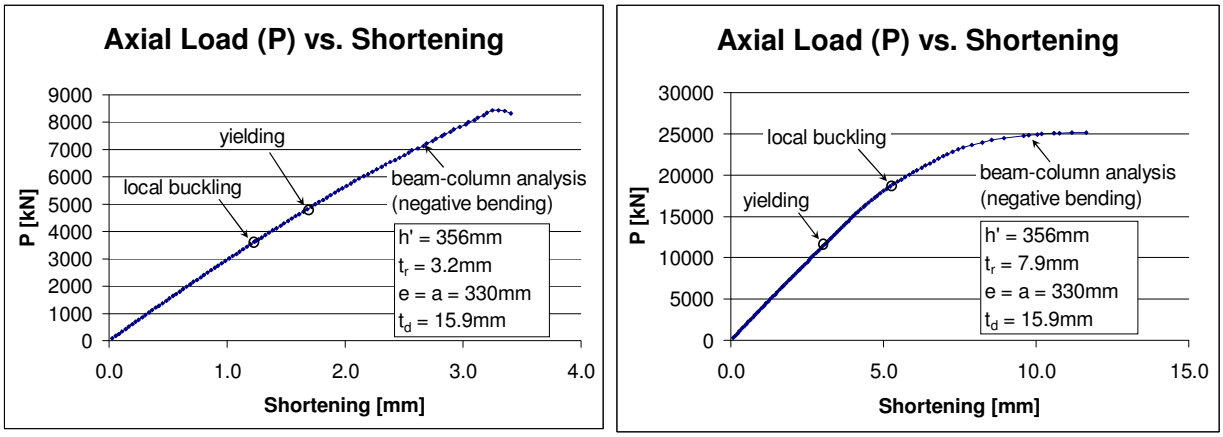

(a) (b)

Figure 11. Load versus deflection curve from beam-column analysis (a) Elastic local buckling of the rib walls (b) Inelastic local buckling of the rib walls.

Figure 11 (a) displays the load versus deflection curve for a deck segment with a slender rib wall (t_r = 3.2mm (1/8")). The width-to-thickness ratio of the rib walls ($h`/t_r$) was large (112). The failure mode was elastic local buckling of the rib walls near the floorbeam at the loaded end of the panel. Local buckling initiated in the rib walls before the development of yield stress anywhere.

Figure 11 (b) shows the load deflection curve for a model with thicker rib members (t_r = 7.9 mm (5/16")) and thus a smaller ratio of rib wall width-to-thickness ($h`/t_r$ = 44.8). The component dimensions are those of the base model. For this particular model the failure mode was inelastic local buckling of the rib walls near the floorbeam at the loaded end of the panel. The load at which local buckling initiated was higher than the load which caused first yielding in the model. The computed deflected shape for this model is shown in Figure 12, which is the typical deflected shape for local buckling in the rib walls under beam-column loading.

The results of varying the thickness of the rib walls of the base model under beam-column loading are presented in Table 2. The axial load at which buckling and yielding initiate are defined as P_{buckle} and P_{yield}, respectively. As expected, thinner rib walls with a large slenderness ratio would buckle locally in the elastic range of material strength while

thicker wall plates, in the inelastic range or could reach global yielding without local buckling.

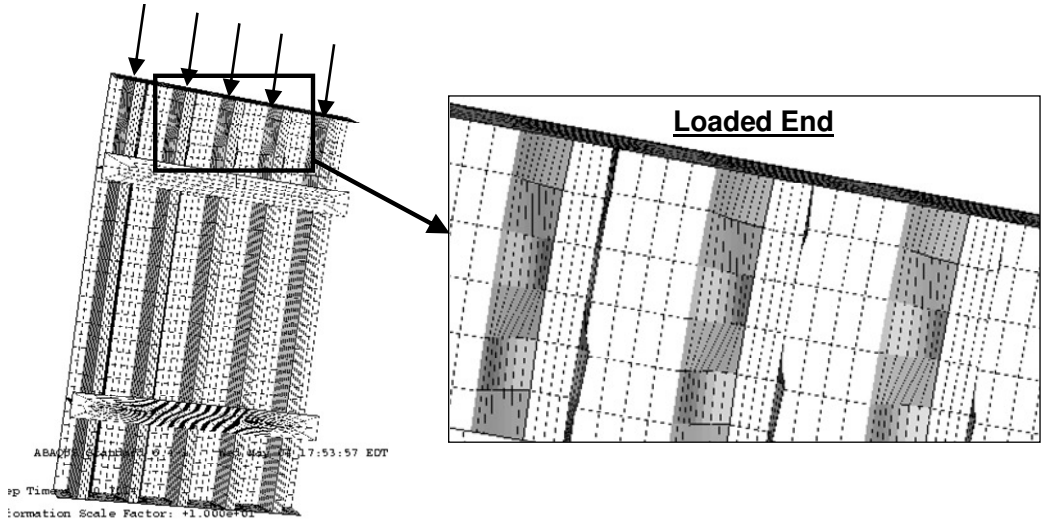

Figure 12. Local buckling of the rib walls looking at the underside of the deck (corresponds with Figure 11 (b))

Table 2. Buckling Loads and Failure Mode

Axial Load with End Moments (Beam - Column Analysis)

t_r	2.4 (3/32)	3.2 (1/8)	4.8 (3/16)	6.4 (1/4)	7.9 (5/16)	9.5 (3/8)
h'/t_r	149.3	112.0	74.7	56.0	44.8*	37.3
P_{buckle}	1486 (334)	3638 (818)	9563 (2150)	14572 (3276)	18922 (4254)	21253 (4778)
P_{yield}	3372 (758)	4817 (1083)	7615 (1712)	9563 (2150)	11689 (2628)	13660 (3071)
FAILURE MODE	Elastic Local Bucklng of Ribs		Inelastic Local Buckling of Ribs			Global Yielding

Units: length in millimeters (inches) and force in kN (kips)

Parameters: h' = 356mm (14"), a = e = 330mm (13"), t_d = 15.9mm (5/8")

Note: metric dimensions approximate (english dimensions exact)

* base model

As mentioned earlier, the slenderness ratio of the deck plate (a/t_d and e/t_d) is typically lower than that of the rib walls ($h`/t_r$). Therefore, under axial compression and negative bending, deck plate local buckling is of much less concern. However, for completeness models of the bridge deck segment under beam-column loading were also analyzed with varying width-to-thickness ratios of the deck plate (a/t_d and e/t_d). Because the compressive stresses were higher in the rib walls than in the deck plate, the models were analyzed with large a/t_d and e/t_d ratios. The resulting behavior was elastic local buckling in the deck plate near the far end of the segment. Then, with decreased a/t_d and e/t_d ratios approaching that

of the width to thickness ratio of the rib walls ($h`/t_r$) inelastic local buckling occurred in the rib walls as shown in Figure 12.

For each case of beam-column analysis the average axial stress at local buckling ($\sigma_{b(avg)}$) was determined. The variation of average axial stresses at local buckling versus the width-to-thickness ratio of the rib walls ($h`/t_r$) and of the deck plate (a/t_d or e/t_d) are compared in Figure 13. These plots show that when the width-to-thickness ratio of the rib walls or the deck plate were decreased, the average axial stresses at local buckling significantly increased. The plots also show that the variation of the average stresses at local buckling were relatively consistent for varied angular rib depth ($h`$) and varied spacing between the ribs (e) or the walls of a rib (a).

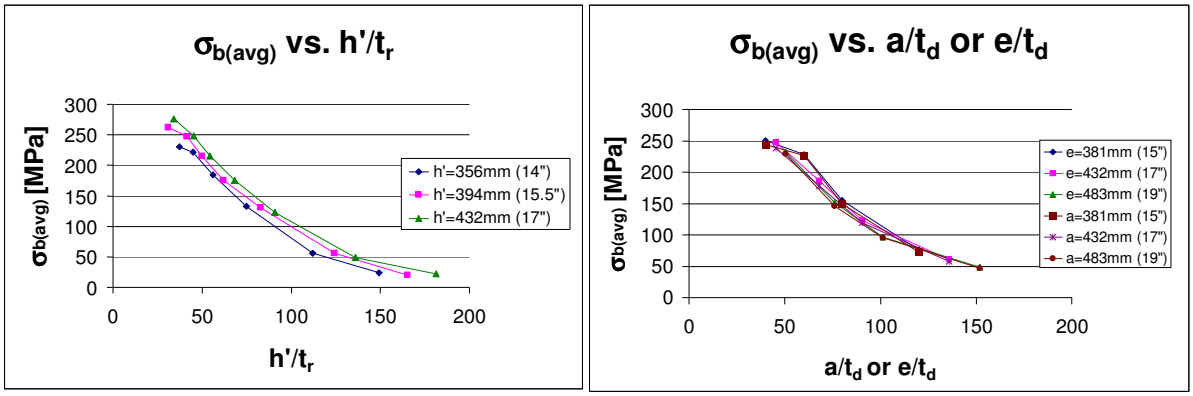

(a) (b)

Figure 13. Average axial stress at local buckling of (a) rib walls ($h`/t_r$) and (b) deck plate (a/t_d or e/t_d)

It is important to note that local buckling of the rib walls or deck plate does not represent the load carrying capacity of the rib. Significant additional load could be carried after local buckling. This can be seen from Figure 11 as an example. The conclusion is different from deck segment models under axial loads only. This is discussed later in the comparison of results (Section 5.3).

5.2 Column analysis

The analysis for designing trapezoidal ribs on orthotropic bridge decks is usually performed under axial compression (column analysis). Figure 14 shows two examples of the load deflection curves obtained from the column analysis of this study.

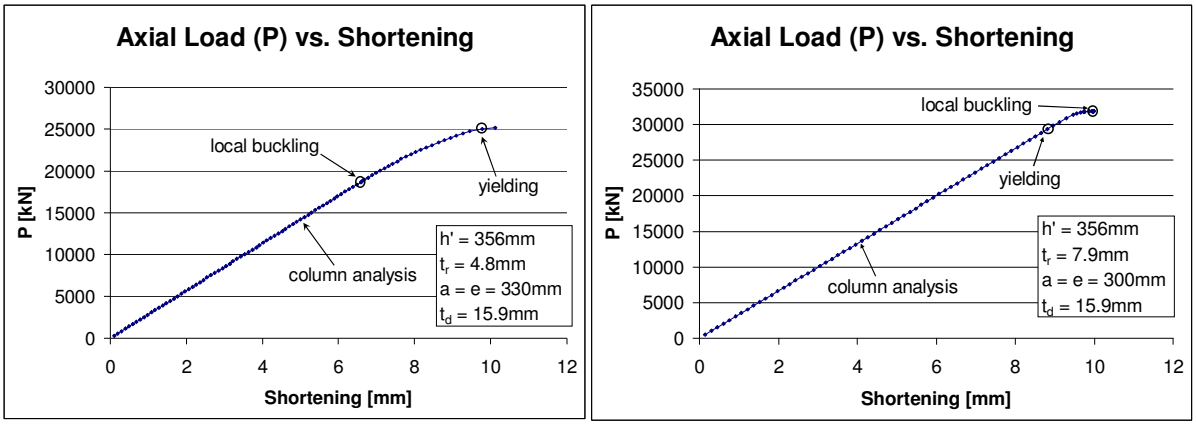

Figure 14. Load versus deflection curve from column analysis (a) elastic local buckling of rib walls (b) inelastic local buckling of rib walls

Figure 14 (a) displays the load versus deflection curve for a deck segment with thin rib walls (t_r = 4.8mm (3/16")). The width-to-thickness ratio of the rib walls was $h`/t_r$ = 74.7. The failure mode was elastic local buckling of the rib walls near mid-span of the deck segment. Figure 14 (b) shows the load deflection curve for the base model with a rib wall thickness of $t_r$ = 7.9mm (5/16") and a slenderness ratio of $h`/t_r$ = 44.8. For this particular model having dimensions of the base model, the failure mode was inelastic local buckling of the rib walls in between the floorbeams and the ends of the segment.

It is to be noted that little additional strength remained after inelastic local buckling of rib wall (Figure 14 (b)).

Table 3 summarizes the computed local buckling loads and yield loads for models of varying rib wall thickness from the base model.

Table 3. Buckling Loads and Failure Mode

Axial Load only (Column Analysis)

t_r	3.2 (1/8)	4.8 (3/16)	5.6 (7/32)	6.0 (15/64)	6.4 (1/4)	7.1 (9/32)	7.9 (5/16)	9.5 (3/8)
h'/t_r	112.0	74.7	64.0	59.7	56.0	49.8	44.8*	37.3
P_{buckle}	9110 (2048)	18726 (4210)	25856 (5813)	27978 (6290)	29041 (6529)	30660 (6893)	31825 (7155)	34121 (7671)
P_{yield}	-	25047 (5631)	26208 (5892)	26919 (6052)	27271 (6131)	28841 (6484)	29851 (6711)	32181 (7235)
FAILURE MODE	Elastic Local Buckling of Ribs			Inelastic Local Buckling of Ribs				Global Yielding

Units: length in millimeters (inches) and force in kN (kips)
Parameters: h' = 356mm (14"), a = e = 330mm (13"), t_d = 15.9mm (5/8")
Note: metric dimensions approximate (english dimensions exact)
* base model

The deck segment was also analyzed for varying deck plate thickness (t_d) (thus varying a/t_d and e/t_d). When a/t_d and e/t_d is smaller than $h`/t_r$ local buckling initiated in the rib walls. For each model analyzed as a column, the average axial stress at local buckling ($\sigma_{b(avg)}$) was

also computed. The variation of the average axial stresses at local buckling versus the width-to-thickness ratio of the rib walls ($h`/t_r$) and of the deck plate (a/t_d and e/t_d) are plotted in Figure 15. This plot shows the variation of stresses at local buckling in the elastic and inelastic range.

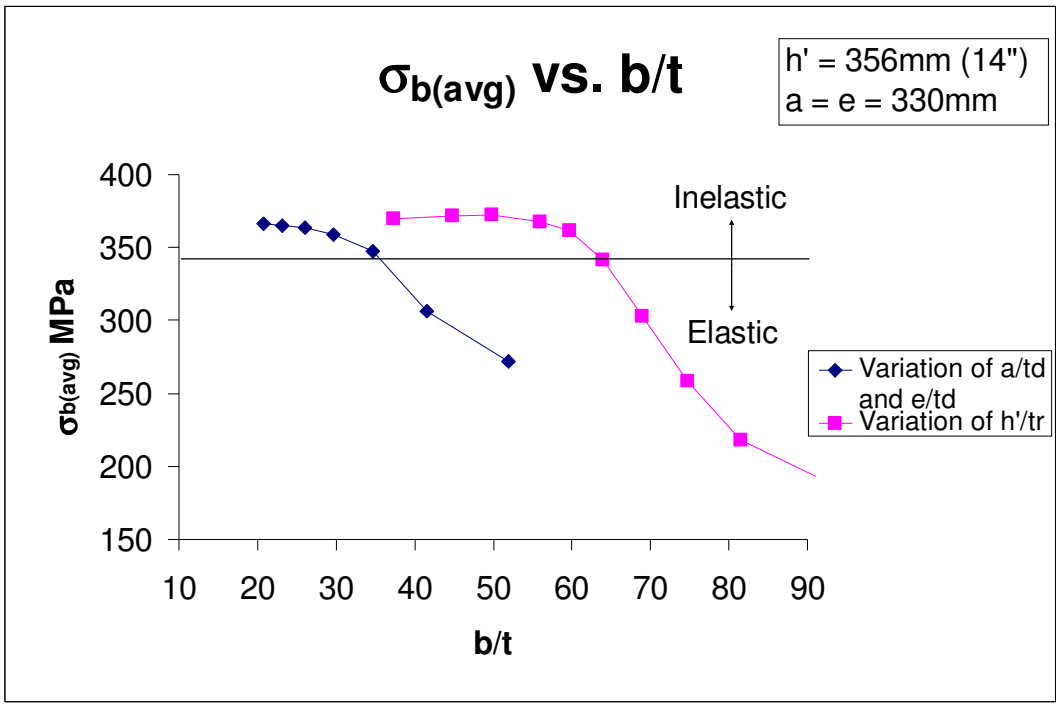

Figure 15. Average axial stress at local buckling versus ($h`/t_r$) and (a/t_d and e/t_d)

5.3 Comparison of results

A comparison between the local buckling behavior of trapezoidal rib orthotropic bridge deck segments under axial load with negative bending moment (beam-column analysis) versus only axial load (column analysis) can be made using the results from finite element analyses as listed in Table 2 and Table 3.

The failure mode and location were generally the same for the beam-column and column analysis. Elastic local buckling initiated in the rib walls of the models when the width-to-thickness ratio ($h`/t_r$) of the ribs was high. As the rib wall thickness increased, local buckling of the walls occurred after the onset of local yielding of the deck segment components. Because of the bending moment in the beam-column analysis, local buckling initiated under a lower load than for the case of column analysis with axial load only. For the base model with component dimensions shown in Figure 7 , these loads were computed to be 18922 kN (4254 kips) and 31825 kN (7155 kips), respectively. The comparison is shown in Figure 16.

As a result, analyzing the deck segment under only axial compression provides an unconservative condition when compared to the loading condition of axial forces with negative bending moment at the end of the rib span as was shown in Figure 4 (c).

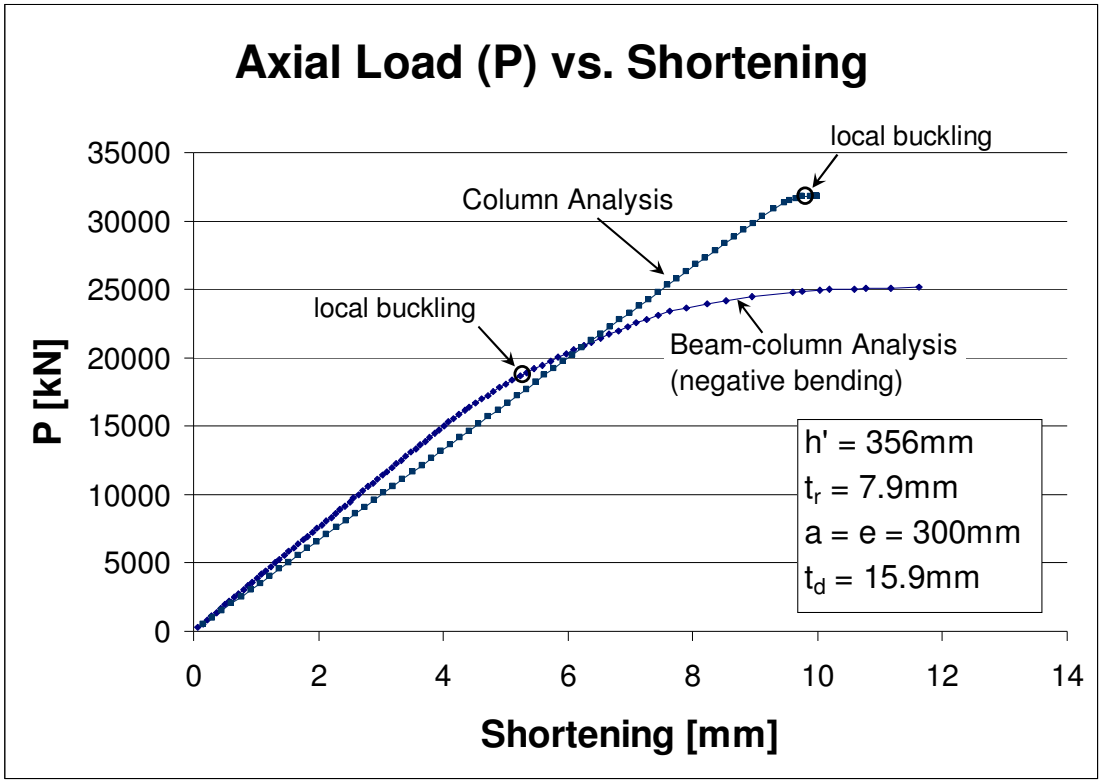

Figure 16. Beam-column analysis versus column analysis of a trapezoidal rib orthotropic bridge deck segment

6. Summary and Conclusions

The important results of this study on local buckling behavior of trapezoidal ribs and deck plates are summarized below.

(1) For the rib walls and deck plate between the rib walls, elastic local buckling occurred when the plate slenderness ratios of these components were high. As the plate thickness was increased (and the corresponding plate slenderness ratio decreased), onset of local yielding in the components initiated before local buckling thus local buckling occurred in the inelastic range of behavior. This is the current basis of designing deck components with an adopted pattern of residual stresses.

(2) Since the rib walls in the analysis were typically more slender than the deck plate between rib walls, local buckling primarily initiated at the rib walls.

(3) Local buckling of the components did not denote the load carrying strength of the deck segments. However, the reserve strength beyond inelastic buckling of the models of the analysis differed depending on the geometry of the components.

(4) Because the trapezoidal ribs in orthotropic bridge decks are usually continuous through floorbeams or diaphragms, a negative bending moment due to the weight of the deck and vehicular loads on the deck exists at the ends of the trapezoidal ribs in the deck segments. The local buckling loads of the ribs under this loading condition (beam-column

with negative bending moment) are lower than those due to axial loads alone (column analysis). Therefore, analyzing deck segments under axial loads only is not conservative.

In conclusion, the negative bending moments from localized forces on orthotropic deck segments should be considered in the design of trapezoidal rib members. The presence of negative bending at floorbeam locations adversely affects the local buckling strength of the ribs. It is recommended that bridges with trapezoidal rib orthotropic deck systems subjected to high global compressive forces include the local negative bending moments when investigating local buckling of the rib members.

References

ABAQUS/CAE User's Manual, 2002, (Hibbitt, Karlsson, & Sorensen, Inc.: Pawtucket, RI).

American Association of State Highway and Transportation Officials, *AASHTO LRFD Bridge Design Specifications*, 3rd edition, 2004 (AASHTO: Washington D.C.).

Chen, S.J., Yang, K.C., Inelastic Behavior of Orthotropic Steel Deck Stiffened by U-Shaped Stiffeners, *Thin-Walled Structures.* January 2002, **40**, 537-553.

Chen, W.F., Duan, L., *Bridge Engineering Handbook*, 1999 (CRC Press: New York).

Connor, R.J., A Comparison of the In-Service Response of an Orthotropic Steel Deck Laboratory Studies and Design Assumptions, *Lehigh University*, May 2002.

Galambos, T.V., *Guide to Stability Design Criteria for Metal Structures*, 1998 (John Wiley & Sons, Inc: New York).

Jen, W.C., Yen, B.T., Load Carrying Capacity of Steel Orthotropic Deck with Trapezoidal Shaped Longitudinal Stiffener, *Lehigh University*, Sept. 2006, ATLSS Report No. 06-15.

Jen, W.C., Yen B.T., Stresses in Orthotropic Steel Deck Components due to Vehicular Loads, *ASCE, SEI, Structures Congress*, 2005, New York.

Troitsky, M.S., *Orthotropic Bridge – Theory and Design*, 1987 (The James F. Lincoln Arc Welding Foundation: Cleveland).

Tsakopoulus, P.A. and Fisher J.W. (2005). Full-Scale Fatigue Test of Steel Orthotropic Deck Panel for the Bronx-Whitestone Bridge Rehabilitation, *Bridge Structures*, 2005, **1**, 55-65.

Wolchuk, R., *Design Manual for Orthotropic Steel Plate Beck Bridges*, 1963 (American Institute of Steel Construction: Chicago).